Λ Spectra in 11.6A GeV/c Au-Au Collisions

S. Albergo,[4] R. Bellwied,[12] M. Bennett,[10] D. Boemi,[4] B. Bonner,[9] H. Caines,[8] W. Christie,[1] S. Costa,[4] H. J. Crawford,[10] M. Cronqvist,[10] R. Debbe,[1] J. Engelage,[10] I. Flores,[6] L. Greiner,[10] T. Hallman,[1] G. Hijazi,[12] G. Hoffmann,[11] H. Z. Huang,[2] T. J. Humanic,[8] A. Insolia,[4] P. Jensen,[11] E. G. Judd,[10] K. Kainz,[9] M. Kaplan,[3] S. Kelly,[2] I. Kotov,[8] G. Kunde,[13] P. J. Lindstrom,[6] T. Ljubicic,[1] W. Llope,[9] G. LoCurto,[8] R. Longacre,[1] D. Lynn,[1] L. Madansky,[5] N. Mahzeh,[5] Z. Milosevich,[3] J. M. Mitchell,[1] J. W. Mitchell,[7] S. Nehmeh,[12] C. Nociforo,[4] S. Paganis,[11] S. U. Pandey,[12] R. Potenza,[4] D. E. Russ,[3] A. Saulys,[1] J. Schambach,[11] J. Sheen,[12] E. Sugarbaker,[8] J. Takahashi,[12] J. Tang,[11] A. L. Trattner,[10] S. Trentalange,[2] A. Tricomi,[4] C. Tuvè,[4] J. P. Whitfield,[3] and K. Wilson[12]

[1]*Brookhaven National Laboratory, Upton, New York*
[2]*University of California, Los Angeles, California*
[3]*Carnegie Mellon University, Pittsburgh, Pennsylvania*
[4]*Università di Catania and INFN-Sezione di Catania, Catania, Italy*
[5]*Johns Hopkins University, Baltimore, Maryland*
[6]*Lawrence Berkeley Laboratory, Berkeley, California*
[7]*NASA Goddard Space Flight Center, Greenbelt, Maryland*
[8]*The Ohio State University, Columbus, Ohio*
[9]*Rice University, Houston, Texas*
[10]*Space Science Laboratories, University of California, Berkeley, California*
[11]*University of Texas, Austin, Texas*
[12]*Wayne State University, Detroit, Michigan*
[13]*Yale University, New Haven, Connecticut*

(Received 8 May 2001; published 25 January 2002)

E896 has measured Λ production in 11.6A GeV/c Au-Au collisions over virtually the whole rapidity phase space. The midrapidity p_t distributions have been measured for the first time at this energy and appear to indicate that the Λ hyperons have different freeze-out conditions than protons. A comparison with the relativistic quantum molecular dynamics model shows that while there is good shape agreement at high rapidity the model predicts significantly different slopes of the m_t spectra at midrapidity. The data, where overlap occurs, are consistent with previously reported measurements.

DOI: 10.1103/PhysRevLett.88.062301 PACS numbers: 25.75.Dw

It has long been predicted that strange particle production will be enhanced should a new phase of matter be produced in heavy ion collisions [1]. The strange hyperon yields and distributions are therefore of great interest as an indicator of strange quark production. The experiment 896 measures Λ hyperon production over a wide p_t range and covers nearly the full range in rapidity. While several other AGS experiments have measured Λ production at lower energies and near beam rapidity, E896 is the first to measure midrapidity yields and spectra in 11.6A GeV/c collisions. Extracting the midrapidity yields of strange baryons is important in order to probe the validity of a variety of production models (e.g., thermal [2] or cascade models [3]) which make systematic predictions of particle production. The production yield is strongest at midrapidity and thus measurements in this kinematic range help to differentiate between production mechanisms. It is also at midrapidity that differences in the p_t spectra between particle species are strongest and the applicability of thermal equilibration models [2] can be probed. Hence, systematic comparisons of the midrapidity spectra of strange hyperons measured at SIS, AGS, and SPS allow the heavy ion collision dynamics to be explored in greater detail.

The experiment 896 was designed to search for the H_0 dibaryon [4]. This fixed target experiment measured Au-Au collisions at 11.6A GeV/c at the Brookhaven National Laboratory's Alternating Gradient Synchrotron. The experiment, shown schematically in Fig. 1, consisted of two main tracking detectors: a 144 plane distributed drift chamber (DDC) [5,6] and a 15 plane silicon drift detector array (SDDA) [7,8]. Each plane of the SDDA consisted of a 6.3 cm $\times$ 6.3 cm $\times$ 300 μm silicon drift detector [9]. The whole SDDA was positioned inside a 6.2 T sweeper field approximately 10 cm downstream of

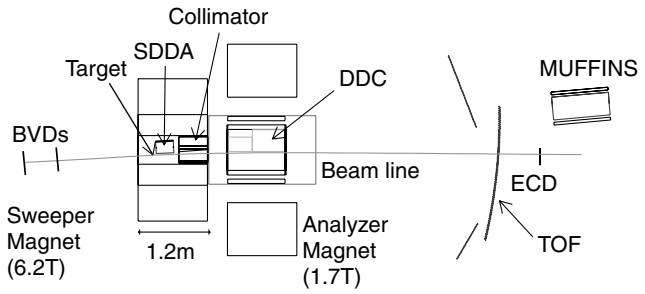

FIG. 1. Schematic diagram of the E896 experimental setup.

the target. The DDC was located with its front face 1.32 m downstream of the target in a 1.6 T analyzing magnet and had an active volume of 120 cm $\times$ 67.5 cm $\times$ 20 cm.

Two beam vertexing detectors (BVDs) were used for locating the primary vertex position and the beam angle. A forward multiplicity array covering the walls of the sweeper magnet, $\sim$30 cm from the target, determined the centrality of the collision. This large acceptance, $1.90 < \eta < 3.33$, photon detector provided a multiplicity measurement for triggering independent of the two tracking devices.

Particle identification is provided by the Multi-Functional Neutron Spectrometer (MUFFINS) [10], used to detect neutrons, and the time-of-flight (TOF) walls, which aid in the definition of the charged tracks reconstructed in the DDC.

The high sweeper magnetic field and collimator mean that only low p_t neutral particles are within the DDC acceptance. This provides a clean environment in which to reconstruct neutral decays such as the $\Lambda \rightarrow p\pi^-$ and the $H_0 \rightarrow \Sigma^- p \rightarrow pn\pi^-$.

For the analysis presented in this paper, 25.5 million of the DDC central events and 350 000 of the SDDA central events were reconstructed. Central events are defined as the top $\sim$5% of the measured signal in the forward multiplicity array. Under the assumption that the measured photon multiplicity is proportional to the cross section which is in turn proportional to the square of the impact parameter it is possible to show that this corresponds to an impact parameter $<= 3$ fm [11].

The Λ hyperon is reconstructed via its decay, with a branching ratio of 64%, into two charged daughters. To identify Λs, all reconstructed negative tracks are combined with all reconstructed positive tracks in the same event. All pairs thus created are examined for a nonprimary vertex, a series of geometric and quality cuts are then applied to reduce the combinatoric background. These cuts consisted of the distance of closest approach to the primary vertex of the secondary daughters, the impact parameter of the parent, the distance of closest approach of the two daughter particles at the secondary vertex, the position of the secondary vertex, and the number of hits on the tracks. The DDC analysis additionally cut on the goodness of fit of the track parametrization, the opening angle of the decay products in the laboratory frame, the momentum of the positive daughter transverse to the parent momentum, to remove photon conversions, and the ratio of the number of hits on the positive track relative to the negative track. This last cut was shown to significantly reduce the combinatoric background produced by wrongly associating primary protons with soft deltas or pions [12]. Additional cuts on the time of flight of each daughter further reduced the background noise [13]. These data sets yielded $\sim$15 000 reconstructed Λs from the SDDA and $\sim$70 000 from the DDC. Good signal to noise ratios of 14:1 and 36:1 and mass widths of 6 and 4 MeV/c^2 in the SDDA and DDC, respectively, are achieved. The SDDA is ideally located to reconstruct Λs at midrapidity over a large p_t range, while the DDC has near-beam rapidity and low p_t acceptance.

A detailed simulation of the experiment using GEANT 3.21 [14] and simulators for each of the tracking detectors were used to calculate the acceptance and efficiency for detection of the Λs and to determine their subsequent momentum resolution [12,15].

Figure 2 shows the corrected transverse mass ($m_t = \sqrt{p_t^2 + m_0^2}$) distributions for Λs reconstructed within the DDC active volume for several rapidity bins from 2.0–3.2. Each bin is scaled by a successive factor of 10 for clarity. Also shown are relativistic quantum molecular dynamics model (RQMD) V2.4 [3] predictions for an impact parameter of 0–3 fm, which is the range comparable to the E896 estimated centrality. It can be seen that the RQMD model reproduces the shape of the measured distributions over the region covered. In Fig. 2 only statistical errors are shown; the systematic error of this data has been estimated to be 15%. The major source of the systematic error comes from the parent Λ, due to finite momentum resolution, being assigned to an incorrect momentum bin and hence having an incorrect efficiency correction applied. The DDC m_t coverage is too small to extract a rapidity density distribution.

Figure 3 shows the corrected m_t distributions for those Λs reconstructed via the SDDA tracking. Again the different rapidity bins are scaled by successive powers of 10 for clarity. Also included, where applicable, are the DDC data. It can be seen that the two independent measurements

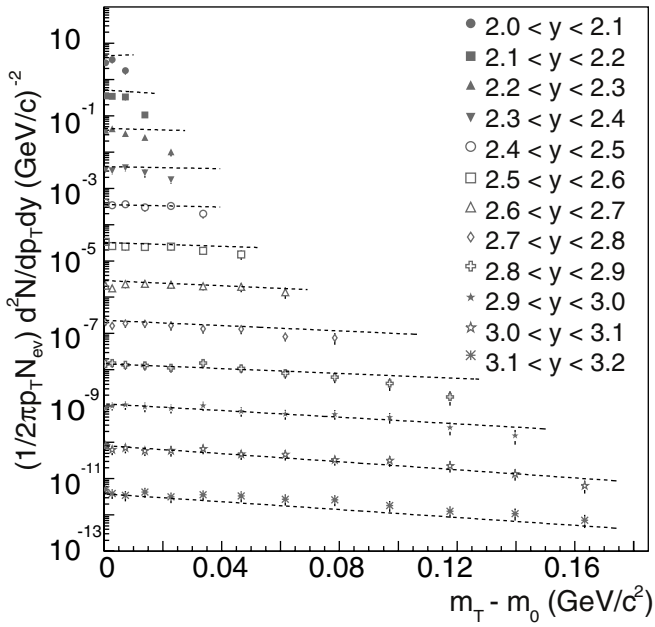

FIG. 2. m_t distributions for DDC Λs. Rapidity slices are scaled by successive factors of 10 for clarity. The lines are the predictions from RQMD.

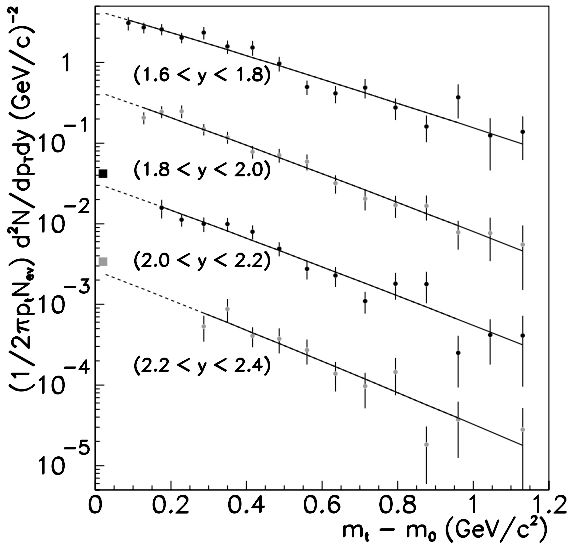

FIG. 3. m_t distributions for SDDA Λs. The lines are fits to Eq. (1), the solid lines indicate the m_t ranges used. Each rapidity bin is scaled by a successive factor of 10 for clarity. Also shown, as solid squares, are the relevant DDC m_t points.

are in good agreement. The m_t distributions were fit to the Boltzmann parametrization [shown in Eq. (1)].

$$\frac{1}{2\pi p_t}\frac{d^2N}{dp_t dy} = A(y) m_t \exp(-m_t/T)\,. \qquad (1)$$

Figure 4 shows the results of these fits as a function of rapidity. The solid points represent the actual fits and the open points a reflection around midrapidity (1.6). Statistical errors only are shown; the systematic error is estimated to be 10%. The systematic error was calculated by

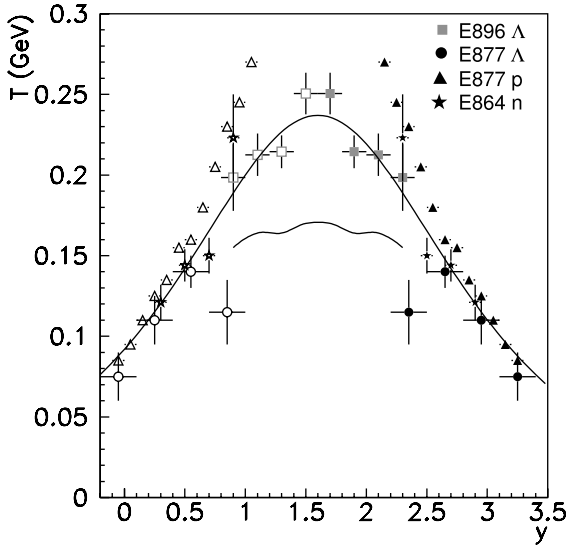

FIG. 4. Inverse slope results as a function of rapidity for SDDA Λs compared to Λ and proton results from E877 [16] and neutron results from E864 [17]. The solid line indicates a fit of the E896 results to Eq. (2) and the dashed line the prediction from RQMD. The solid shapes are the measured points and the open shapes reflections around midrapidity.

studying the sensitivity of the corrected data to applied cuts and to the ranges used in the fits to the m_t distributions. This study identified the major source of the SDDA systematic error to be the uncertainty in the primary vertex location. The primary vertex resolution was shown to be 2.8 mm in x, the bend plane, and 1 mm in y; the z position was assumed in aligning the detectors and magnetic field [15]. An error in the primary vertex results in the impact parameter of the daughter and parent particles being incorrectly calculated. As the impact parameters are important for increasing the signal-to-noise ratio these variables cannot be ignored and hence a study was made using Monte-Carlo simulations to estimate the effect of the primary vertex uncertainty in the Λ reconstruction as a function of p_t and rapidity. It was shown that the systematic error introduced has some p_t dependence, the higher p_t bins being more strongly affected by an error in the vertex calculation than the lower p_t Λs, and also an overall shift in the calculated efficiency as a function of p_t and rapidity. High momentum Λs and their daughters point back more strongly to the primary vertex and hence are more sensitive to small variations in the calculated position. This results in a systematic error in the calculated inverse slope. Both the p_t dependence and overall shift result in a larger systematic error in the calculated yields, estimated to be 20%, than in the inverse slope measurements. If one assumes an isotropic source it can be shown that the inverse slope parameters should show a $1/\cosh(y)$ dependence. Indeed a fit to Eq. (2) of the E896 SDDA data shows our Λs are in good agreement with this simple model with a midrapidity inverse slope ($T_{\rm cm}$), as defined by Eq. (2), of 237 ± 5 MeV

$$T = \frac{T_{\rm cm}}{\cosh(y - y_{\rm CM})} \qquad (2)$$

Also shown in Fig. 4 are previous Λ and proton measurements in Au-Au collisions at the same energy and similar centrality [16] as well as neutron results from 11.5A GeV/c Au-Pb collisions with a 10% centrality [17]. It can be seen that there is good agreement between the two Λ data sets where overlap occurs, and that there appears to be a consistent trend from midrapidity to near beam values which is well reproduced by the fit to Eq. (2). The dashed line represents a fit to the cascade RQMD prediction; it can be seen that the model consistently underpredicts the inverse slopes near midrapidity. Fits to the RQMD simulation were made only in the m_t and rapidity ranges measured, hence any distortions due to the detector's limited phase space acceptance should be reproduced in the RQMD fits.

However, the slope parameters of the Λs are seen to have a different trend than that for the proton/neutron as a function of rapidity. Near beam rapidity the proton and Λ results are similar, but for the data near midrapidity the proton inverse slopes show much higher values than the Λ spectra at the same rapidity. This is consistent with a

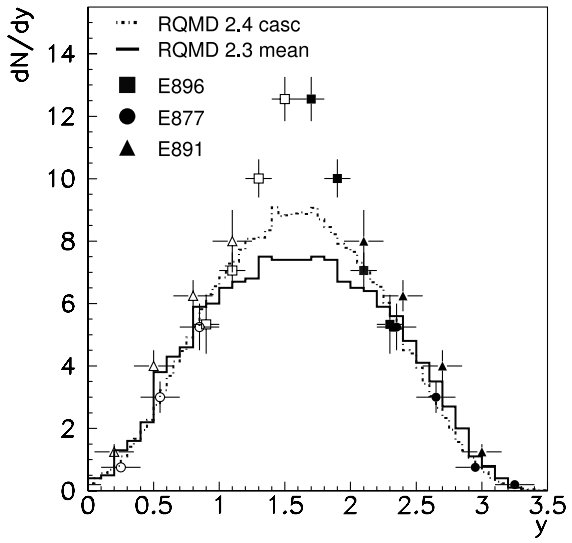

FIG. 5. Rapidity distribution for SDDA Λs. The solid points are measured and the empty shapes are reflections around midrapidity. Also shown are data points reported by E877 [16] (circles) and E891 [20] (triangles). The solid and dashed lines are RQMD predictions.

picture that protons suffer stronger final state interactions resulting in a transverse flow larger than that of the Λs. A similar idea has been previously suggested to explain the Ω results at the SPS [18]. The observation that Λs and protons may have different space-time emission characteristics has been previously suggested by E895 [19] for Au-Au collisions at 6*A* GeV where they also note that the Λ, K_s^0, and proton p_t spectra cannot be described by a unique temperature and radial flow velocity.

It is possible to extract the rapidity density for Λs using the fitted p_t distributions extrapolated to regions where the detector had no coverage. Shown in Fig. 5 is the resultant dN/dy distribution with only statistical errors plotted. Also shown in Fig. 5 are previous measurements by E891 [20] and E877 [16] and the predictions from RQMD using both the mean field and cascade calculations. It can be seen that neither calculation reproduces the data well at midrapidity. Integration of all the available Λ measurements gives a yield of 16.7 ± 0.5 (stat) Λs per central Au-Au collision ~80% of which is covered by the E896 data.

In summary, the data presented here agree well with the previously reported experimental data where overlap occurs. At high rapidity both the cascade and mean field calculations predict similar shapes, however at midrapidity neither calculation reproduces the E896 data. The total yield of Λs per central event, as calculated from all the experimental data, is in agreement with the RQMD prediction.

The inverse slopes as measured by the SDDA are consistent with other experiments where there is overlapping coverage. A comparison of the inverse slopes to previous proton data appears to indicate that the Λ hyperons at 11.6*A* GeV/c collisions have less transverse flow than the protons. There have been previous indications of this from E895 at lower AGS energies. A comparison with RQMD indicates, however, that the Λs experience more transverse flow than the model predicts especially at midrapidity.

We wish to thank the AGS Operations group of the Brookhaven National Laboratory for their support in performing this experiment. The work was supported by the Division of Nuclear Physics of the Office of Science of the U.S. Department of Energy, the United States National Science Foundation, and the Brazilian FAPESP–Fundação de Amparo à pesquisa do estado de São Paulo.

[1] P. Koch, B. Muller, and J. Rafelski, Phys. Rep. **142**, 167 (1986).
[2] J. Stachel, Nucl. Phys. **A610**, 509C (1996).
[3] H. Sorge, Phys. Rev. C **52**, 3291 (1995).
[4] R. L. Jaffe, Phys. Rev. Lett. **38**, 195 (1977).
[5] E896 Collaboration, M. Kaplan *et al.,* Adv. Nucl. Dyn. **3**, 205 (1997).
[6] E896 Collaboration, S. Albergo *et al.,* Lawrence Berkeley National Laboratory Report No. LBNL-47409, 2001 (unpublished).
[7] J. Takahashi *et al.,* Nucl. Instrum. Methods Phys. Res., Sect A **453**, 131 (2000).
[8] J. Takahashi *et al.,* Nucl. Instrum. Methods Phys. Res., Sect A **439**, 497 (2000).
[9] E. Gatti and P. Rehak, Nucl. Instrum. Methods Phys. Res., Sect A **225**, 608 (1984).
[10] S. Albergo *et al.,* Nucl. Instrum. Methods Phys. Res., Sect A **311**, 280 (1992).
[11] G. Lo Curto, Ph.D. thesis, The Ohio State University, 1999.
[12] S. Kelly, Ph.D. thesis, University of California, Los Angeles, 2000.
[13] K. Kainz, Ph.D. thesis, Rice University, 2001.
[14] R. Brun *et al.,* GEANT Detector Description and Simulation Tool, CERN Program Library (1993).
[15] J. Sheen, Ph.D. thesis, Wayne State University, 2000.
[16] E877 Collaboration, J. Barrette *et al.,* Phys. Rev. C **63**, 014902 (2001).
[17] E864 Collaboration, T. Armstrong *et al.,* Phys. Rev. C **60**, 064903 (1999).
[18] H. van Hecke, H. Sorge, and N. Xu, Phys. Rev. Lett. **81**, 5764 (1998).
[19] E895 Collaboration, P. Chung *et al.,* in *Proceedings of Strangeness 2000* [J. Phys. G **27**, 293 (2001)].
[20] E891 Collaboration, S. Ahmed *et al.,* Phys. Lett. B **382**, 35 (1996).